Biotechnology Notes 4 (2023) 83–89

Contents lists available at ScienceDirect

Biotechnology Notes

journal homepage: www.keaipublishing.com/en/journals/biotechnology-notes/

Suitability evaluation of toehold switch and EXPAR for cell-free MicroRNA biosensor development

Caroline E. Copeland [a], Yong-Chan Kwon [a,b,*]

[a] Department of Biological and Agricultural Engineering, Louisiana State University, Baton Rouge, LA, 70803, USA
[b] Louisiana State University Agricultural Center, Baton Rouge, LA, 70803, USA

ARTICLE INFO

Keywords:
Cell-free system
MicroRNA
Biosensor
Toehold switch
Exponential amplification reaction

ABSTRACT

The development of a robust and cost-effective sensing platform for microRNA (miRNA) is of paramount importance in detecting and monitoring various diseases. Current miRNA detection methods are marred by low accuracy, high cost, and instability. The toehold switch riboregulator has shown promising results in detecting viral RNAs integrated with the freeze-dried cell-free system (CFS). This study aimed to leverage the toehold switch technology and portability to detect miRNA in the CFS and to incorporate the exponential amplification reaction (EXPAR) to bring the detection to clinically relevant levels. We assessed various EXPAR DNA templates under different conditions to enhance the accuracy of the sensing platform. Furthermore, different structures of toehold switches were tested with either high-concentration synthetic miRNA or EXPAR product to assess sensitivity. Herein, we elucidated the mechanisms of the toehold switch and EXPAR, presented the findings of these optimizations, and discussed the potential benefits and drawbacks of their combined use.

1. Introduction

MicroRNA (miRNA) has been highlighted as an important type of biomarker for various diseases. Recent studies have confirmed that the dysregulation of miRNA can be correlated with the development and specific stage of major diseases, multiple cancer types,[1–5] viral infections,[6–9] diabetes,[10–13] and cardiovascular diseases.[14–16] However, current miRNA detection methods often necessitate expensive equipment and resources, and they are plagued by low detection accuracy attributed to miRNA vulnerability.[17–19] Consequently, there is an increasing demand for novel technologies in the form of on-demand, cost-effective miRNA sensors, owing to their potential to facilitate the detection and monitoring of various disease diagnoses and prognoses in non-laboratory environments. Most of the non-conventional low-cost methods rely on miRNA hybridization to an RNA or DNA in both the amplification and detecting modules.[17,20] This nucleic acid hybridization technique is the core concept of the toehold switch riboregulator, which has shown great success in detecting viral RNAs integrated with a portable and low-cost cell-free system (CFS).[21] While the CFS's portability and cost-effectiveness as a biosensor make it a promising candidate for microRNA detection, the potential for it to serve as a robust and accurate miRNA detection platform remains unexplored in the context of toehold switches for miRNA detection.

The toehold switch is a programmable RNA sensor that detects the sequence of interest on the sample's RNA called the trigger RNA. The synthetic riboregulators use toehold-mediated linear-linear RNA-RNA interactions designed *in vitro* that initiate strand displacement interactions.[22] Once the trigger RNA binds to the target strand, the switch releases a sequestered ribosome binding site and a start codon to initiate the translation of a colorimetric or fluorescent reporter protein to verify if the RNA sequence of interest is present (Fig. 1A). Nucleic acid sequence-based amplification (NASBA) is a pre-step isothermal amplification reaction[23] technique that is known to be fast and sensitive and has been used for diagnostics in field-based settings[24] as well as used with the toehold switch to bring femtomolar RNA concentration amounts in samples up to detectable levels.[21] However, since typical 18–24 nucleotide-long miRNAs do not comply with the length of the primer standards for the amplification, NASBA remains an unfeasible approach to amplify the miRNA up to a detectable amount that can operate the toehold switch.[21,25]

Abbreviations: miRNA, microRNA; CFS, cell-free system; NASBA, nucleic acid sequence-based amplification; EXPAR, exponential amplification reaction; NEase, nicking endonuclease; NUPACK, nucleic acid package; DTT, dithiothreitol; ANOVA, analysis of variance; Tm, melting temperature; PEG, polyethylene glycol; SSB, single-strand binding protein.

* Corresponding author. Department of Biological and Agricultural Engineering, Louisiana State University, Baton Rouge, LA, 70803, USA.
E-mail address: yckwon@lsu.edu (Y.-C. Kwon).

https://doi.org/10.1016/j.biotno.2023.11.003
Received 7 August 2023; Received in revised form 12 November 2023; Accepted 13 November 2023
Available online 17 November 2023

On the other hand, exponential amplification reaction (EXPAR) facilitates isothermal miRNA amplification using short DNA oligonucleotides with half of the oligo binding to the target miRNA and the other half serving as a template to create multiple copies once triggered. This method can reach a high amplification of $>10^6$-fold in a short period of time (<30 min).[26] The reaction relies on a linear template containing two repeat regions (X′-X′) that are complementary to the trigger (target) sequence (X). These regions are separated by a short nicking endonuclease (NEase) recognition region. First, the trigger X anneals to the X′ region on the 3′ end of the template allowing for the 3′ end of the trigger to be exposed. The trigger itself acts as a primer, and a DNA polymerase binds to the 3′ end of the trigger extending the strand to the end of the other X′ region. Then, the NEase creates a nick at the cleavage site, causing DNA polymerase to start displacing identical trigger strands on the newly made 3′ end (Fig. 1B).[26,27] Despite the advantageous high amplification of target miRNA, EXPAR suffers from background amplification.[28] Niemz et al. showed that the EXPAR DNA template itself was one of the main generators of the background noise, and when the template sequence was changed, the background changed simultaneously.[28,29] The main factors contributing to background amplification included 3′ end extension resulting from intramolecular or intermolecular template-template non-specific binding, as well as the general non-specific binding of nucleic acids.[26]

Here, we investigated the effects of combining EXPAR and the toehold switch in the CFS to develop a miRNA biosensor. This combination will allow for the removal of a fluorescent reader, such as a qPCR machine, and offer more portability and ease of use to the test. We studied methods of reducing background amplification from EXPAR by comparing five different modified DNA templates, reaction temperatures, and crowding agents. The reaction conditions that showed the largest reduction of the background was chosen to be introduced to the toehold switch CFS compared to a high concentration of synthetic miRNA (miR-335-5p) (Fig. 1C). miR-335-5p was chosen as it has previously been reported to be a potential oncogenic biomarker related to its tumor suppressive role.[30] Two versions of toehold switches were tested with varying sequences to optimize the ratio of leak to ease of triggering. With these combinations, a robust, low-cost, and accurate miRNA detection system was expected to be created. Throughout the studies, we observed the limitations of EXPAR to accurately amplify the miRNA and the necessary toehold switch response to the present miRNA. These methods both operate based on nucleic acid hybridization, so we presume the core problem lies with the difficulty of hybridizing short AU-rich miRNA sequences. However, these discoveries are important to share for future research, as miRNA sensing is becoming a popular biosensing technique with most technologies focusing on hybridization.

2. Materials and methods

2.1. In silico design

The toehold switches were designed *in silico* to detect miR-335-5p, with similar characteristics to the toehold switch series B design from Pardee et al.[21] Using NUPACK software, the optimal free energy and any conflicts of the secondary structure were found (Fig. S2).[31] Sequences were constructed to be complementary to the miRNA target, form the toehold switch in the correct fashion desired, and ensure there were no stop codons or frameshifts after the start codon in the linker region. EXPAR templates were designed to include a complementary binding region, a nicking region, and another region for the polymerase to make identical copies of the miRNA in double-stranded DNA form. The genes were synthesized from Integrated DNA Technologies (IDT, Coralville, IA) with different template modifications (biotinylated and phosphorothioate additions) chosen in the settings of the IDT's online builder. Synthetic single-stranded miRNA-335-5p was also synthesized from IDT.

2.2. EXPAR

EXPAR was conducted as specified by Zhang et al.[32] with slightly modified reaction components. The reaction was 20 μL in total, comprising of Mixture A and Mixture B. Mixture A contained trigger (synthetic single-stranded miRNA-335-5p), 0.2 μM amplification template, 1x NEBuffer 3.1, and 500 μM dNTPs. Mixure B contains 1x IsothermoPol buffer, 0.5 U/μL Nt.BstNBI nicking endonuclease, 0.5 U/μL Bst DNA polymerase, 2x EvaGreen®, and 2x ROX reference dye. Mixture A and Mixture B were prepared separately on ice, and then they were

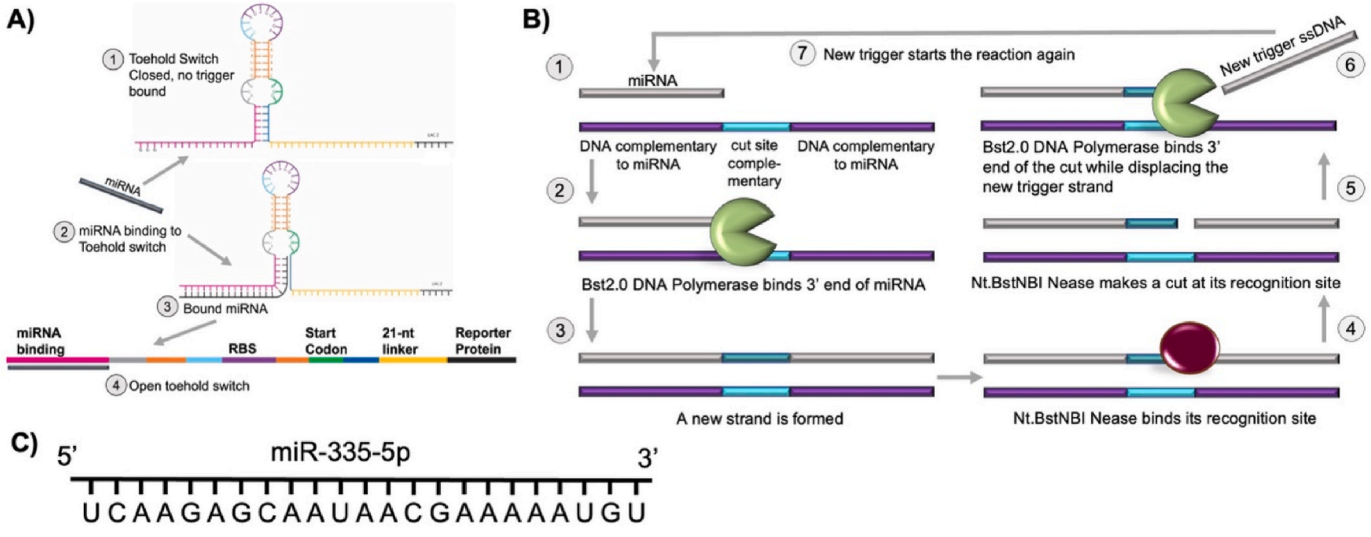

Fig. 1. Combination of toehold switch and exponential amplification reaction for miRNA detection A) Structure of toehold switch. Once a complementary RNA molecule binds to the unsequestured region (step 3), it opens the switch by continued base pairing within the toehold (step 4). The opened toehold switch releases the start codon and ribosome binding site (RBS) to initiate reporter protein translation. **B)** EXPAR process. The trigger X (miRNA) anneals to the X′ region on the 3′ end of the template allowing for the 3′ end of the trigger to be exposed (step 1). The trigger itself acts as a primer, and a DNA polymerase binds to the 3′ end of the trigger extending the strand to the end of the other X′ region (steps 2–3). NEase creates a nick at the cut site (steps 4–5), causing DNA polymerase to come to the newly made 3′ end and displace the identical trigger strands (step 6). The displaced strand becomes a new trigger which can then start another reaction, and the initial trigger can start the reaction again on the same template strand (steps 7-1). **C)** Sequence of synthetic miRNA-355-5p (5' – 3′).

pre-heated separately to 55 °C before combining Mixture B into Mixture A. The fluorescence output was measured at a minute interval using the qPCR machine (Bio-Rad, Hercules, CA) immediately. The qPCR machine was set to run at 55 °C for 70 cycles. Streptavidin was added to Mixture A containing the biotinylated templates with a final concentration of 2 μM in Mixture A + B. Single-strand binding protein from Sigma-Aldrich (S3917) was added at the final concentration (in Mixture A + B reaction) of 2 μM to Mixture A as described.[26] Polyethylene Glycol (PEG 8000, Thermo Fisher Scientific, Waltham, MA) was added to Mixture A at a final concentration of 2 % in the Mix A + B reaction. All enzymes and ROX reference dye were purchased from New England Biolabs (Ipswich, MA).

2.3. Recombinant plasmid

The toehold switch was added to the pJL1-*sfGFP* vector following the standard Gibson Assembly method. The recombinant plasmid was then transformed into DH5alpha *Escherichia coli* competent cells via electroporation and selected on an LB agar plate containing Kanamycin (50 μg/mL). Colonies were screened by colony PCR, and subsequent Sanger sequencing confirmed the sequences. The recombinant plasmid was then purified at a high concentration (200 μg/mL) using the plasmid preparation kit (Qiagen, Germantown, MD).

2.4. Cell-extract preparation

The *E. coli* strain BL21 Star™ (DE3) (genotype F- *ompT hsdS*$_B$ (r_B-, m_B-) *gal dcm rne131* (DE3)) (Invitrogen, Waltham, MA) was used for the cell-extract for the cell-free protein synthesis reaction. The cell-extract was prepared as described previously.[33] In brief, the cells were grown in 2xYTPG media in shake flasks at 37 °C with vigorous shaking (250 rpm). The cells were harvested OD_{600} at 3.0 and washed three times with the chilled Buffer A (10 mM Tris-acetate (pH 8.2), 14 mM magnesium acetate, 60 mM potassium acetate, and 2 mM DTT). The cells were then resuspended in Buffer A (without DTT) and lysed by sonication. The cell-extract was aliquoted out, flesh frozen in liquid nitrogen, and stored in −80 °C freezer until use.

2.5. Cell-free reactions with toehold switch

Cell-free reaction mixtures were prepared as described previously.[34] The standard 15 μL cell-free reaction mixture in a 1.7 mL microtube includes BL21 Star™ (DE3) cell-extract (4 μL), 1 μL salt solution (12 mM magnesium glutamate, 10 mM ammonium glutamate, and 130 mM potassium glutamate), 1.2 mM ATP, 0.85 mM each of GTP, UTP, and CTP, 34 μg/mL L-5-formyl-5,6,7,8-tetrahydrofolic acid (folinic acid), 170 μg/mL E. *coli* total tRNA, 57 mM HEPES buffer (pH 7.2), 0.4 mM nicotinamide adenine dinucleotide (NAD), 0.27 mM coenzyme A, 4 mM sodium oxalate, 1 mM putrescine, 1.5 mM spermidine, 2 mM each of 20 canonical amino acids, 33 mM phosphoenolpyruvate (PEP), and 13.3 μg/mL plasmid. The cell-free reaction microtubes were then incubated at 37 °C for 20 h. Synthetic single-stranded miRNA-335-5p, EXPAR product from miRNA, or EXPAR background product from no miRNA present were inserted into the cell-free reaction with the toehold switch plasmid. Negative control reactions included the cell-free reaction mixture with either synthetic single-stranded miRNA, EXPAR product, or EXPAR background product with no plasmid DNA containing the toehold switch and sfGFP gene.

2.6. Statistical analysis

Statistical analyses were conducted using GraphPad Prism 8.4.3 (GraphPad Software) with a 5 % significance level. For the parametric analysis of data from the fluorescent measurements from synthesized sfGFP, two-way ANOVA was used.

3. Results and discussion

3.1. Template type and temperature study for reducing background

Biotinylation and phosphorothioate modifications of the EXPAR DNA template have previously been shown to reduce background amplification. Biotinylated EXPAR templates reduce the melting temperature (T_m) of the primer/template duplex.[35–37] If the T_m of the 5′ end is lower than that of the 3′ end, then there will be faster dissociation of the miRNA from the 5′ end, allowing more amplification reactions to occur since there will be more circulating miRNA to pair with the correct end, the 3′ end.[35] Possibly, biotinylation on both ends of the template will help avoid non-specific binding in general because the template will rely heavier on exact free energies from the Watson-Crick interaction for binding, and the lower T_m will encourage the incorrectly paired sequence to dissociate faster.[35] In addition, streptavidin assists in decreasing the *Tm* of the duplex by 10 °C.[36] It is believed that this decrease in Tm is due to steric repulsion between the protein and the binding site of the major groove of the DNA helix.[36] Protection of DNA template degradation has also been found with the addition of biotin and streptavidin.[37] Phosphorothioate modifications to the 5' end of the template have shown promising results in reducing background amplification, mainly by protecting the DNA template from degradation.[38–43] A recent study discovered that bacterial post-transcriptional phosphorothioate modification positioned at a designated cleavage site or next to one can prevent digestion by the endonuclease.[44] The phosphorothioate modification functions by replacing non-bridging oxygen in the DNA sugar-phosphate backbone with a sulfur atom.[45]

Five different non-modified and modified (biotinylation and phosphorothioate) EXPAR templates were tested to find out if the template modification had a significant impact on reducing background amplification. We also investigated the addition of streptavidin to the biotinylated templates (T4 and T5), as well as the range of reaction temperatures, to find the optimal condition showing the greatest delay of background amplification (Fig. 2). The templates include a standard EXPAR template (T1), three consecutive phosphorothioate bonds on the 3′ end only (T2), three consecutive phosphorothioate bonds on the 3′ end and three on the 5′ end (T3), a biotinylated tag on the 5′ end only (T4), and biotinylated tags on the 3′ and 5' end (T5) (Fig. 2A). T2 was the only template that had a significant time delay between the true signal output and background amplification, with a 15.2 and 12.3 min delay between 1 nM and 0.1 nM of synthetic miRNA, respectively (Fig. 2B and Fig. S3). However, reactions with all templates, including T2, showed high variance in amplification time of the true signal output and the background signal, making it difficult to determine when to stop the amplification reaction to avoid the potential background signal generation. For example, in the T2 reactions, even though the background is on average 12–15 min away from the true signal, the reaction event time varies by 5.6 min, 2.1 min, and 10 min for 1 nM and 0.1 nM, and 0 nM of synthetic miRNA, respectively.

Raw fluorescence readings over time that were observed in qPCR output (Fig. S3) indicate that post-initiation, the reaction progresses exponentially, culminating in a plateau of fluorescence intensity. Critical to our understanding is the temporal aspect of reaction onset. It is hypothesized that higher concentrations of miRNA would precipitate an earlier reaction onset, whereas the absence of miRNA would result in a significantly delayed response or none at all. To accurately obtain and communicate the variations observed across repeated experiments under the same conditions, we calculated the time delay in amplification between the true signal and the background noise. Consequently, we utilized minimum, mean, and maximum value plots as more informative alternatives to qPCR amplification plots in this study.

When streptavidin was added to bind to the biotinylated templates (T4 and T5) to reduce the melting temperature of the oligo regions, there still was not a noticeable time difference of amplification between the true sample (1 nM miRNA) and background (0 nM miRNA) but a delay of

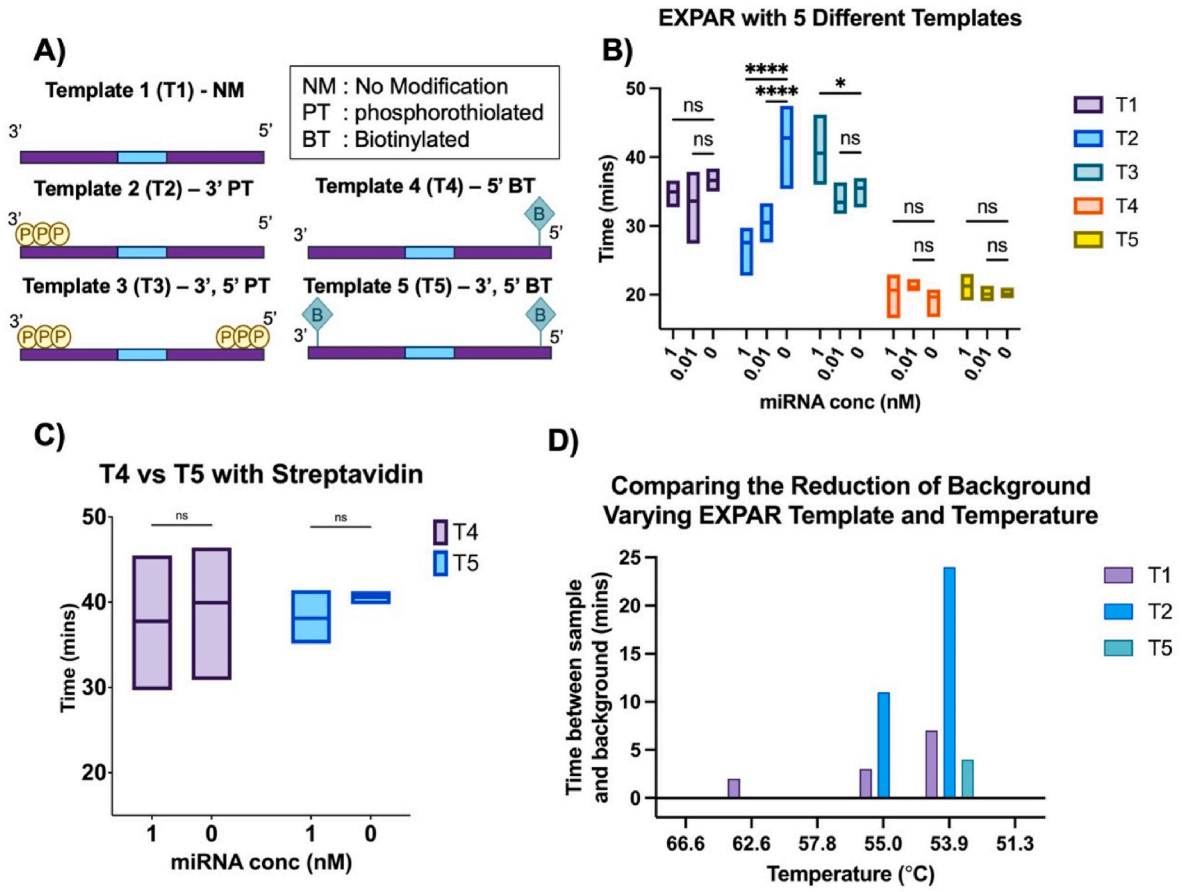

Fig. 2. EXPAR template types and temperature comparison. A) Five EXPAR template modifications. **B)** Measuring background delay depending on miRNA concentration and template type. Values represented as mean, min & max, n = 3, ****p < 0.0001, *p < 0.5. **C)** The addition of streptavidin to the biotinylated templates showed no significant delay of background amplification **D)** Effects of background delay depending on temperature and template showing more delay.

reaction from both groups compared to no streptavidin was observed (Fig. 2C). Finally, we observed a large reduction of the background signal for templates T1, T2, and T5 at 53.9 °C, which was 1.1 °C lower than the standard reaction temperature (55 °C) (Fig. 2D and Fig. S4). This phenomenon could be due to the reduction of temperature, allowing easier complete binding of the synthetic miRNA.

3.2. *Molecular crowding and single-strand binding protein*

Research has found that adding small molecules to serve as crowding agents has improved the EXPAR performance, specifically single-stranded binding protein (SSB) and ethylene glycol.[26,46,47] We decided to test the background-reducing effects of SSB as well as introduce another small molecule, polyethylene glycol (PEG), which has shown promising results in other isothermal nucleic acid amplification reactions.[48] Macromolecules occupy 20–30 % of the cells' interiors and macromolecule crowding generates thermodynamic and kinetic effects on the cell's functions.[49,50] When a spherical macromolecule occupies a space, the effective volume of occupancy is 8 times its intrinsic volume because it excludes other molecules from taking up that space and this increases thermodynamic activity. Brownian motion creates unsymmetrical forces from the contact of molecules on molecules.[51] These forces increase the volume available to the macromolecules and satisfy the second law of thermodynamics by favoring maximum entropy. Molecular interactions under entropic forces could be more readily reversible than those caused by ionic forces (e.g., DNA condensed by PEG is more flexible and less compacted than when it is condensed by electrostatic interactions), thus encouraging the cell to correct mistakes, and possibly enabling the correct nucleic acid hybridization interactions in the EXPAR reaction.[51] SSB is a widely used protein that binds to single-stranded DNA (ssDNA). SSB can not only protect the unpaired ssDNA from degradation but inhibit secondary structure formation.[26]

The crowding effect was tested by introducing PEG (2 %) and SSB (2 μM) into the EXPAR reaction. The EXPAR fluorescence output was measured at 1-min intervals using a qPCR machine. First, we found PEG allowed for a slight reduction of background signal in the T5 template compared to 0 % crowding, but not a significant difference compared to the present (1 nM) and absent (0 nM) of the synthetic miRNA (Fig. 3A). In a separate experiment comparison, the amplification results of the combination of PEG and T5 were inconsistent, showing large variability across experiments with EXPAR in general that has been observed (Fig. 3B). However, 2 % of PEG induced a modest reduction of the background signal with the T2 template (Fig. 3B). Unfortunately, we observed successive result inconsistencies when comparing the results of another EXPAR reaction (Fig. 3C). This trend of inconsistency with the ability to differentiate low concentrations of miRNA from background amplification is an unattractive characteristic of EXPAR for miRNA sensing and amplification use. The substantial increase (x1000 times, 1 nM to 1 μM) of miRNA concentration input induced a noticeable signal output time difference with the T2 template (Fig. 3C). However, this concentration (1 μM) is not a good comparison for a direct serum sample, with total levels of miRNA in serum near 10 ng/mL.[52] In addition, using this large concentration of miRNA did allow for a closer look at the crowding effect on the reaction, with SSB addition exhibiting a significant decrease in the background whereas PEG increased background amplification (Fig. 3C).

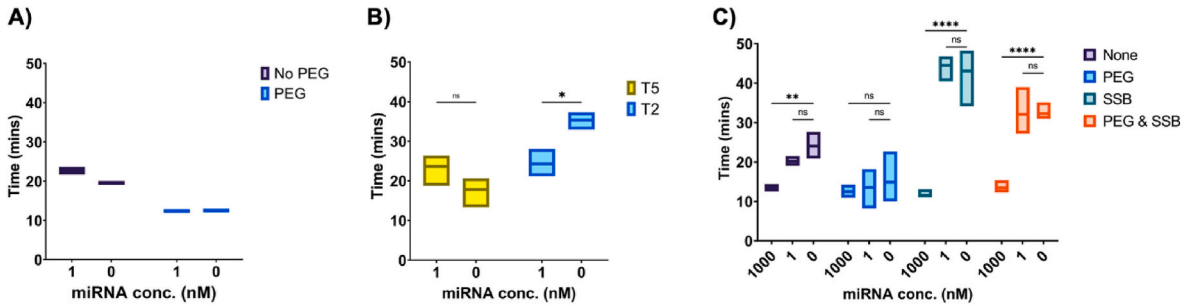

Fig. 3. Effect of crowding agent and single-strand binding protein. A) T5 biotin template background reduction with and without crowding reagent (PEG). **B)** Reduced background under crowding conditions with biotinylated T2 and T5 templates. **C)** Combination of PEG and SSB on excessive miRNA concentration with T2 template. Values represented as mean, min & max, n = 3, ****p < 0.0001, **p < 0.01, *p < 0.5.

3.3. Failed toehold switch reactions and miRNA hybridization binding energy

Once the miRNA is amplified from the low concentration found in human serum, it should be able to be detected in the CFS miRNA sensing platform by triggering the toehold switch, giving a colorimetric output. When designing the toehold switch sequence elements, Pardee et al. used thermodynamic considerations to optimize the design by reducing the ribosome binding site contained loop sequence, further stabilizing the stem sequence of the sensor by adding extra nucleotides and removing the downstream refolding domain. In contrast to 18–24 nt short miRNAs, target-specific toehold switch optimization is a rational process with relatively lengthier target viral RNA strands. These factors have a large impact on decreasing leakage of false ON states (false positive) while increasing the free energy required to unwind the sensor,[21] making it more of a challenge to tailor the toehold switch for miRNA triggers. Overall, their optimal toehold switch design contains a leader sequence of three guanines to encourage efficient transcription by T7 RNA polymerase, the exposed complementary trigger section (around 12 nt), a sequestered 9 nt continuation of the complementary sequence to the trigger, a conserved sequence region which contains the sequestered start codon in a 3 nt bulge and the sequestered RBS in a 12 nt loop, an exposed 21 nt low-weight amino acid coding sequences, and the protein of interest sequence.[21,22]

Based on the optimal parameters of the original toehold switch from Pardee et al., two versions (V1 and V2) of the toehold switch were designed. Switch V1 was designed to match the optimal parameters exactly. Switch V2 was designed based off of Pardee et al.'s studies showing a loop elongation to 24 nt provides a considerable effect on increasing signal while keeping false triggering remains low. CFS reactions were carried out using 100 μM of synthetic miRNA, EXPAR product, or EXPAR background amplification product. The true EXPAR product was taken from the previously optimized reaction: 1 μM of miRNA, three consecutive phosphorothioate modifications on the 3′ end only (T2), and SSB. The reaction was then stopped after the expected true amplification detection and before generating the background amplification. The EXPAR background amplification product was taken from the EXPAR reaction with the same characteristics minus the miRNA trigger. It was allowed to run for 60 min for background amplification to occur. CFS reaction controls included miRNA or EXPAR input without toehold switch DNA, thus no fluorescence from the CFS should occur. Unfortunately, neither the synthetic 100 μM miRNA trigger nor the EXPAR product was able to trigger either version of the toehold switch, as shown by the lack of fluorescent change compared to the controls (Fig. 4).

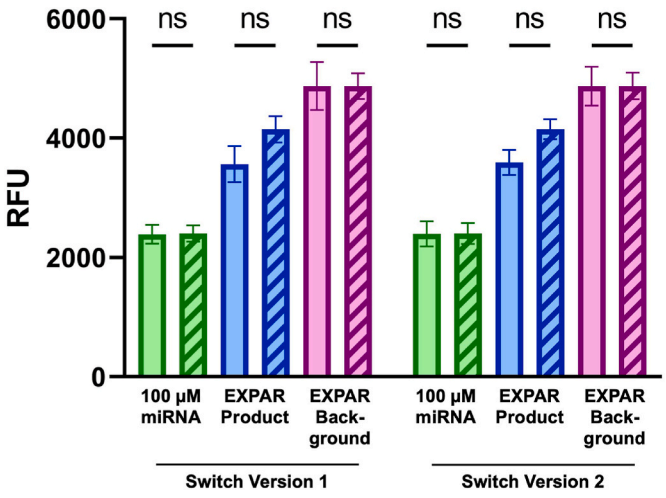

Fig. 4. Toehold switch performance in the CFS. (Solid bars) Cell-free reaction with the synthetic miRNA at high concentration (100 μM), EXPAR product, or EXPAR background amplification product. (Pattern bars) Control reactions: Cell-free reaction containing no toehold DNA with no reporter fluorescent protein gene. Values are represented as mean ± SD.

4. Conclusion

The intrinsic open nature of the CFS allows the system to easily transform into a versatile *in vitro* biomarker-sensing platform. The combination of the isothermal amplification triggered by the miRNA of interest from EXPAR, and a programmable toehold switch in the CFS providing an easy-to-read colorimetric output, could in theory provide a low-cost and accessible miRNA detection system. However, due to the short length and low GC contents of matured miRNA, once bound to the toehold switch trigger, there are not enough nucleotides in the unbound state to attribute to base-pair stacking and other thermodynamics of the nucleic acid strand to counteract the repulsion caused by the negatively charged phosphate backbone.[53–55] This results in weak hybridization to the binding region of the toehold switch and a lack of energy to operate the toehold switch.

The same principles can be used to account for EXPAR's pitfalls, except for weak or incomplete binding causes false activation. miRNA, EXPAR products, or other free-floating EXPAR templates can bind incompletely to the binding region of the EXPAR template, causing an activation of the DNA polymerase even if the binding event is short-lived. Once the DNA polymerase is activated and displaces the complementary sequence to the binding region, the EXPAR product will be increased by 2^n. Since this inaccurate EXPAR triggering is a random event, the reaction termination before the background signal generation cannot be relied on because it can occur at different times for different individual runs. There is also no alternative method to differentiate the background signal from the true sample signal output by end-point quantification using a qPCR machine, since they both will occur until the reaction runs to completion once triggered. The reaction conditions

can only be reliable if the background amplification is removed completely.

In order to accomplish miRNA sensing, various new ideas have been suggested in the past few years, including isothermal amplification, electrochemical methods, enzymatic and other biochemical reactions, and nanoparticles.[56–58] Unfortunately, the aforementioned approaches also resulted in relatively higher false positive rates,[19] and the problem of inadequate specificity still exists. Specificity is the key to making an accurate diagnosis or prognosis of various diseases by miRNA detection due to high homology across miRNA sequences.[56] However, many of the existing miRNA detection methods heavily rely on base-pairing of the short, single-stranded, mature miRNAs. Such hybridization methods lead to problems where a probe only partly binds to a miRNA, making it difficult to determine the accuracy of a putative signal.[56]

In conclusion, utilizing EXPAR and the toehold switch in the CFS for miRNA sensing was not considered an optimal combination for the development of an accurate miRNA detection platform. Nonetheless, this study proposed a preliminary idea and framework to navigate the research guideline for designing miRNA detection platforms.

Author contributions

C.E.C. and Y.-C.K. conceived the contents. C.E.C. conducted the experiments. C.E.C. and Y.-C.K. analyzed the data C.E.C. wrote the original manuscript. C.E.C. and Y.C.-K. revised and edited the manuscript. All authors contributed to the article and approved the submission version.

Declaration of competing interest

The authors declare no competing financial interest.

Acknowledgements

This work was supported by the LSU LIFT^2 Fund (Grant No. AG-2022-LIFT-002) and the USDA National Institute of Food and Agriculture HATCH fund (Accession No. 1021535, Project No. LAB94414).

Appendix A. Supplementary data

Supplementary data to this article can be found online at https://doi.org/10.1016/j.biotno.2023.11.003.

References

1. Qi J, Wang J, Katayama H, Sen S, Liu SM. Circulating microRNAs (cmiRNAs) as novel potential biomarkers for hepatocellular carcinoma. *Neoplasma*. 2013;60(2):135–142.
2. Iorio MV, Ferracin M, Liu CG, et al. MicroRNA gene expression deregulation in human breast cancer. *Cancer Res*. 2005;65(16):7065–7070.
3. Iorio MV, Visone R, Di Leva G, et al. MicroRNA signatures in human ovarian cancer. *Cancer Res*. 2007;67(18):8699–8707.
4. Porkka KP, Pfeiffer MJ, Waltering KK, Vessella RL, Tammela TL, Visakorpi T. MicroRNA expression profiling in prostate cancer. *Cancer Res*. 2007;67(13):6130–6135.
5. Calin GA, Liu CG, Sevignani C, et al. MicroRNA profiling reveals distinct signatures in B cell chronic lymphocytic leukemias. *Proc Natl Acad Sci U S A*. 2004;101(32):11755–11760.
6. Luna JM, Scheel TK, Danino T, et al. Hepatitis C virus RNA functionally sequesters miR-122. *Cell*. 2015;160(6):1099–1110.
7. Chen AK, Sengupta P, Waki K, et al. MicroRNA binding to the HIV-1 Gag protein inhibits Gag assembly and virus production. *Proc Natl Acad Sci U S A*. 2014;111(26):E2676–E2683.
8. Jopling CL, Yi M, Lancaster AM, Lemon SM, Sarnow P. Modulation of hepatitis C virus RNA abundance by a liver-specific MicroRNA. *Science*. 2005;309(5740):1577–1581.
9. Anadol E, Schierwagen R, Elfimova N, et al. Circulating microRNAs as a marker for liver injury in human immunodeficiency virus patients. *Hepatology*. 2015;61(1):46–55.
10. Nielsen LB, Wang C, Sorensen K, et al. Circulating levels of microRNA from children with newly diagnosed type 1 diabetes and healthy controls: evidence that miR-25 associates to residual beta-cell function and glycaemic control during disease progression. *Exp Diabetes Res*. 2012;2012, 896362.
11. Liu Y, Gao G, Yang C, et al. The role of circulating microRNA-126 (miR-126): a novel biomarker for screening prediabetes and newly diagnosed type 2 diabetes mellitus. *Int J Mol Sci*. 2014;15(6):10567–10577.
12. Yang Z, Chen H, Si H, et al. Serum miR-23a, a potential biomarker for diagnosis of pre-diabetes and type 2 diabetes. *Acta Diabetol*. 2014;51(5):823–831.
13. Hathaway QA, Pinti MV, Durr AJ, Waris S, Shepherd DL, Hollander JM. Regulating microRNA expression: at the heart of diabetes mellitus and the mitochondrion. *Am J Physiol Heart Circ Physiol*. 2018;314(2):H293–H310.
14. Wojciechowska A, Braniewska A, Kozar-Kaminska K. MicroRNA in cardiovascular biology and disease. *Adv Clin Exp Med*. 2017;26(5):865–874.
15. Zampetaki A, Mayr M. MicroRNAs in vascular and metabolic disease. *Circ Res*. 2012;110(3):508–522.
16. Philippen LE, Dirkx E, da Costa-Martins PA, De Windt LJ. Non-coding RNA in control of gene regulatory programs in cardiac development and disease. *J Mol Cell Cardiol*. 2015;89(Pt A):51–58.
17. Dave VP, Ngo TA, Pernestig A-K, et al. MicroRNA amplification and detection technologies: opportunities and challenges for point of care diagnostics. *Lab Invest*. 2019;99(4):452–469.
18. Gillespie P, Ladame S, O'Hare D. Molecular methods in electrochemical microRNA detection. *Analyst*. 2019;144(1):114–129.
19. Ye J, Xu M, Tian X, Cai S, Zeng S. Research advances in the detection of miRNA. *J Pharm Anal*. 2019;9(4):217–226.
20. Khandan-Nasab N, Askarian S, Mohammadinejad A, Aghaee-Bakhtiari SH, Mohajeri T, Kazemi Oskuee R. Biosensors, microfluidics systems and lateral flow assays for circulating microRNA detection: a review. *Anal Biochem*. 2021;633,114406.
21. Pardee K, Green AA, Takahashi MK, et al. Rapid, low-cost detection of Zika virus using programmable biomolecular components. *Cell*. 2016;165(5):1255–1266.
22. Green AA, Silver PA, Collins JJ, Yin P. Toehold switches: de-vovo-designed regulators of gene expression. *Cell*. 2014;159(4):925–939.
23. Guatelli JC, Whitfield KM, Kwoh DY, Barringer KJ, Richman DD, Gingeras TR. Isothermal, in vitro amplification of nucleic acids by a multienzyme reaction modeled after retroviral replication. *Proc Natl Acad Sci U S A*. 1990;87(5):1874–1878.
24. Cordray MS, Richards-Kortum RR. Emerging nucleic acid–based tests for point-of-care detection of malaria. *Am J Trop Med Hyg*. 2012;87(2):223–230.
25. Deiman B, van Aarle P, Sillekens P. Characteristics and applications of nucleic acid sequence-based amplification (NASBA). *Mol Biotechnol*. 2002;20(2):163–179.
26. Reid MS, Paliwoda RE, Zhang H, Le XC. Reduction of background generated from template-template hybridizations in the exponential amplification reaction. *Anal Chem*. 2018;90(18):11033–11039.
27. Van Ness J, Van Ness, L K, Galas DJ. Isothermal reactions for the amplification of oligonucleotides. *Proc Natl Acad Sci U S A*. 2003;100(8):4504–4509.
28. Tan E, Erwin B, Dames S, et al. Specific versus nonspecific isothermal DNA amplification through thermophilic polymerase and nicking enzyme activities. *Biochemistry*. 2008;47(38):9987–9999.
29. Qian J, Ferguson TM, Shinde DN, et al. Sequence dependence of isothermal DNA amplification via EXPAR. *Nucleic Acids Res*. 2012;40(11):e87.
30. Ye L, Wang F, Wu H, et al. Functions and targets of miR-335 in cancer. *OncoTargets Ther*. 2021;14:3335–3349.
31. Zadeh JN, Steenberg CD, Bois JS, et al. NUPACK: analysis and design of nucleic acid systems. *J Comput Chem*. 2011;32(1):170–173.
32. Zhang K, Kang D-K, Ali MM, et al. Digital quantification of miRNA directly in plasma using integrated comprehensive droplet digital detection. *Lab Chip*. 2015;15(21):4217–4226.
33. Kwon Y-C, Jewett MC. High-throughput preparation methods of crude extract for robust cell-free protein synthesis. *Sci Rep*. 2015;5:8663.
34. Kim J, Copeland CE, Padumane SR, Kwon YC. A crude extract preparation and optimization from a genomically engineered Escherichia coli for the cell-free protein synthesis system: practical laboratory guideline. *Methods Protoc*. 2019;2(3):68.
35. Chen J, Zhou X, Ma Y, Lin X, Dai Z, Zou X. Asymmetric exponential amplification reaction on a toehold/biotin featured template: an ultrasensitive and specific strategy for isothermal microRNAs analysis. *Nucleic Acids Res*. 2016;44(15):e130.
36. Zhang Z, Hejesen C, Kjelstrup MB, Birkedal V, Gothelf KV. A DNA-mediated homogeneous binding assay for proteins and small molecules. *J Am Chem Soc*. 2014;136(31):11115–11120.
37. Wu Z, Wang H, Guo M, Tang L-J, Yu R-Q, Jiang J-H. Terminal protection of small molecule-linked DNA: a versatile biosensor platform for protein binding and gene typing assay. *Anal Chem*. 2011;83(8):3104–3111.
38. Murgha YE, Rouillard J-M, Gulari E. Methods for the preparation of large quantities of complex single-stranded oligonucleotide libraries. *PLoS One*. 2014;9(4), e94752.
39. Wang L, Chen S, Jiang S, Deng Z, Dedon PC. DNA phosphorothioate modification—a new multi-functional epigenetic system in bacteria. *FEMS Microbiol Rev*. 2018;43(2):109–122.
40. Gish G, Eckstein F. DNA and RNA sequence determination based on phosphorothioate chemistry. *Science*. 1988;240(4858):1520.
41. Stein CA. Exploiting the potential of antisense: beyond phosphorothioate oligodeoxynucleotides. *Chem Biol*. 1996;3(5):319–323.
42. Powers A, Carbone M. The role of environmental carcinogens, viruses, and genetic. *Cancer Biol Ther*. 2002;1(4):347–352.
43. Volk DE, Lokesh GLR. Development of phosphorothioate DNA and DNA thioaptamers. *Biomedicines*. 2017;5(3):41.
44. Chen C, Wang L, Chen S, et al. Convergence of DNA methylation and phosphorothioation epigenetics in bacterial genomes. *Proc Natl Acad Sci U S A*. 2017;114(17):4501.

45. Wang L, Chen S, Xu T, et al. Phosphorothioation of DNA in bacteria by dnd genes. *Nat Chem Biol*. 2007;3(11):709–710.
46. Mok E, Wee E, Wang Y, Trau M. Comprehensive evaluation of molecular enhancers of the isothermal exponential amplification reaction. *Sci Rep*. 2016;6, 37837.
47. Wang J, Zou B, Rui J, et al. Exponential amplification of DNA with very low background using graphene oxide and single-stranded binding protein to suppress non-specific amplification. *Microchim Acta*. 2015;182(5):1095–1101.
48. Özay B, McCalla SE. A review of reaction enhancement strategies for isothermal nucleic acid amplification reactions. *Sens Actuators Rep*. 2021;3, 100033.
49. Ellis RJ. Macromolecular crowding: obvious but underappreciated. *Trends Biochem Sci*. 2001;26(10):597–604.
50. Minton AP. The Influence of macromolecular crowding and macromolecular confinement on biochemical reactions in physiological media. *J Biol Chem*. 2001;276(14):10577–10580.
51. Hancock R. Crowding, entropic forces, and confinement: crucial factors for structures and functions in the cell nucleus. *Biochemistry (Mosc)*. 2018;83(4):326–337.
52. Mompeón A, Ortega-Paz L, Vidal-Gómez X, et al. Disparate miRNA expression in serum and plasma of patients with acute myocardial infarction: a systematic and paired comparative analysis. *Sci Rep*. 2020;10(1):5373.
53. Searle MS, Williams DH. On the stability of nucleic acid structures in solution: enthalpy - entropy compensations, internal rotations and reversibility. *Nucleic Acids Res*. 1993;21(9):2051–2056.
54. Yakovchuk P, Protozanova E, Frank-Kamenetskii MD. Base-stacking and base-pairing contributions into thermal stability of the DNA double helix. *Nucleic Acids Res*. 2006;34(2):564–574.
55. Joo C, Rueda D. *Biophysics of RNA-Protein Interactions: A Mechanistic View*. New York: Springer-Verlag; 2019:249. vol. II.
56. Ouyang T, Liu Z, Han Z, Ge Q. MicroRNA detection specificity: recent advances and future perspective. *Anal Chem*. 2019;91(5):3179–3186.
57. Zhu C-s, Zhu L, Tan D-a, et al. Avenues toward microRNA detection in vitro: a review of technical advances and challenges. *Comput Struct Biotechnol J*. 2019;17:904–916.
58. Kilic T, Erdem A, Ozsoz M, Carrara S. MicroRNA biosensors: opportunities and challenges among conventional and commercially available techniques. *Biosens Bioelectron*. 2018;99:525–546.